frontiers in Immunology

ORIGINAL RESEARCH
published: 28 September 2021
doi: 10.3389/fimmu.2021.740540

IL-17$^+$ Mast Cell/T Helper Cell Axis in the Early Stages of Acne

Yoan Eliasse[1,2†], *Edouard Leveque*[1,2†], *Lucile Garidou*[3], *Louise Battut*[1,2], *Brienne McKenzie*[1,2], *Thérèse Nocera*[4,5], *Daniel Redoules*[3] *and Eric Espinosa*[1,2*]

[1] Inserm, U1037, Centre de Recherche en Cancérologie de Toulouse (CRCT), Toulouse, France, [2] Université de Toulouse, Université Paul Sabatier, Toulouse, France, [3] Department of Pharmacology, Pierre Fabre Dermo-Cosmétique, Toulouse, France, [4] Clinical Evaluation Center, Pierre Fabre Dermo-Cosmétique, Toulouse, France, [5] Dermatology Department, University Hospital Larrey, Toulouse, France

Acne is a multifactorial disease driven by physiological changes occurring during puberty in the pilosebaceous unit (PSU) that leads to sebum overproduction and a dysbiosis involving notably *Cutibacterium acnes*. These changes in the PSU microenvironment lead to a shift from a homeostatic to an inflammatory state. Indeed, immunohistochemical analyses have revealed that inflammation and lymphocyte infiltration can be detected even in the infraclinical acneic stages, highlighting the importance of the early stages of the disease. In this study, we utilized a robust multi-pronged approach that included flow cytometry, confocal microscopy, and bioinformatics to comprehensively characterize the evolution of the infiltrating and resident immune cell populations in acneic lesions, beginning in the early stages of their development. Using a discovery cohort of 15 patients, we demonstrated that the composition of immune cell infiltrate is highly dynamic in nature, with the relative abundance of different cell types changing significantly as a function of clinical lesion stage. Within the stages examined, we identified a large population of CD69$^+$ CD4$^+$ T cells, several populations of activated antigen presenting cells, and activated mast cells producing IL-17. IL-17$^+$ mast cells were preferentially located in CD4$^+$ T cell rich areas and we showed that activated CD4$^+$ T cells license mast cells to produce IL-17. Our study reveals that mast cells are the main IL-17 producers in the early stage of acne, underlying the importance of targeting the IL-17$^+$ mast cell/T helper cell axis in therapeutic approaches.

Keywords: mast cells, IL-17, Th17, acne (acne vulgaris), immune landscape, IL17-dependent inflammation

OPEN ACCESS

Edited by:
Wanjun Chen,
National Institutes of Health (NIH),
United States

Reviewed by:
Craig L Maynard,
University of Alabama at Birmingham,
United States
Noa B. Martin-Cofreces,
Princess University Hospital, Spain

***Correspondence:**
Eric Espinosa
eric.espinosa@inserm.fr

†These authors have contributed equally to this work

Specialty section:
This article was submitted to T Cell Biology, a section of the journal Frontiers in Immunology

Received: *14 July 2021*
Accepted: *02 September 2021*
Published: *28 September 2021*

Citation:
Eliasse Y, Leveque E, Garidou L, Battut L, McKenzie B, Nocera T, Redoules D and Espinosa E (2021) IL-17$^+$ Mast Cell/T Helper Cell Axis in the Early Stages of Acne. Front. Immunol. 12:740540. doi: 10.3389/fimmu.2021.740540

INTRODUCTION

Acne vulgaris is a chronic inflammatory skin disease that appears concomitantly with hormonal changes at puberty and constitutes the most common cutaneous disorder in adolescents and young adults. It affects the skin pilosebaceous units, which consist of the hair shaft and the hair follicle with an attached sebaceous gland. Excess sebum and hyperkeratinisation plug up the pore, leading to dramatic changes in the PSU microenvironment (1).

Abbreviations: APC, antigen presenting cell; CC, closed comedone; DC, dendritic cell; hMC, primary human mast cell line; iDC, inflammatory dendritic cell; ILC, innate lymphoid cell; MPO, myeloperoxidase, PA, papule; PCA, Principal component analysis; PSU, pilosebaceous unit; SIS, skin immune system, Tconv, conventional T cells; TRM, resident memory T cell, UI, uninvolved skin.

The pathogenesis of acne is not fully understood. Hormonal stimuli at puberty induce sebocyte and ductal keratinocyte activation and proliferation in the PSU, leading to hyperproduction of sebum and disturbed keratinization (1). Sebum accumulation and progressive clogging of the pore create a new environment that impacts the PSU microbiota and notably foster *C. acnes* proliferation. Ensuing cellular stress and disruption in homeostasis provide several pro-inflammatory cues. These changes, in combination with other factors that remain to be elucidated, drive a naive PSU into the acne cycle (2) starting with the microcomedone stage. Microcomedones are histological observations, invisible by eye, that can be detected by skin surface biopsy (3). Next the microcomedone evolves into a closed comedone (CC or whitehead) or open comedone. These stages are associated with a lack of visible inflammation. While some lesions remain as comedones and resolve, others evolve toward an exacerbation of the inflammatory process leading to the first visible inflamed lesions named papules (PA). These latter lesions can regress or evolve toward pustule and subsequently nodule and/or cyst (1, 2, 4).

The early changes that occur inside a PSU and underlie the progression through the CC stage and next through the PA stage are poorly understood. Notably, the role of the skin immune system (SIS) remains subject to much debate. The early immune response observed in acne is only partially described and appears to be different from the classical inflammatory response mounted against a pathogen, in which the early steps are dominated by neutrophil and subsequently monocyte infiltration upon danger/pathogen recognition. Pioneering histology studies of skin biopsies reported that T lymphocytes were the first cells to infiltrate early lesions (5–7). Moreover, some T cells infiltrating early stages of acne were found to be specific for *C. acnes* antigens (8). A consensus has now developed suggesting that the inflammatory response observed after the PA stage first emerges in the very early stages of the disease (4) and that inflammation is the starting point of the acne process. Nevertheless, the immune surveillance system of the skin is complex (9, 10) and several resident sentinel cells (dendritic cells, macrophages and mast cells) might be involved in perceiving the alarm signals and in starting the early response. Mast cell are particularly abundant in skin and mucosa and are strategically located near blood vessels and nerve endings (11). They can produce a large array of mediators and respond to perturbations in their environment, leading to their involvement in several inflammatory disorders (11, 12). Whilst the role of mast cells in acne is poorly understood, these cells are known to play important roles in the skin immune system (13). Furthermore, different resident and recirculating T cell subsets are also known to participate in immune surveillance of the skin (14) and might be involved in the initiation of the immune response in acne. *C. acnes* is an extracellular pathogen expected to induce a type 3 immune response orchestrated mainly by Th17 cells (15). IL-17 and related cytokines are proinflammatory cytokines known to promote anti-microbial protective responses and barrier maintenance but also pathogenic inflammation upon chronic activation (16). IL-17 (17) and Th17 cells (18, 19) were reported to be associated with acne pathogenesis but their functional role in acne remains understudied.

To gain a more comprehensive understanding of the early inflammatory response in lesions, we profiled the evolution of skin immune cell populations during the early stages of acne (CC and PA). Using a global approach combining flow cytometry, confocal microscopy, and bioinformatics, we highlighted that multiple immune cell populations are swiftly recruited and that the evolving nature of these immune populations is a defining feature of lesion stage. Microscopy approaches allowed us to identify that mast cells were the main IL-17 producers in the CC stage and that mast cell IL-17 production was licensed by activated $CD4^+$ T cells. Our study thus provides unprecedented insight into the immune events that shape early lesion development and identify potential targets for therapeutic intervention.

MATERIAL AND METHODS

Skin Biopsies

15 young male adults with acne on the back (phototype II to IV), presenting Investigator Global Assessment score ≥ 3, were enrolled in the study. Main exclusion criteria included: presence of any skin condition that would interfere with the diagnosis or assessment of acne vulgaris, sun exposure, anti-inflammatory treatments, topical acne or antibiotic treatments within 14 days prior to baseline, use within 1 month prior to baseline of systemic antibiotics, use within 6 months prior to baseline of oral retinoids. Patients gave written informed consent under a protocol approved by local ethic committee (CCP Sud-ouest et Outremer III, #Id RCB: 2015-A01858-41) an in agreement with the Declaration of Helsinki Principles. Punch biopsies (3 biopsies of 4mm and 2 biopsies of 3 mm diameter) were taken from the back of the patients (**Supplementary Figure 1**). Biopsies were stored in buffer (MACS Tissue Storage Solution, Miltenyi Biotec) at 4°C and processed within 2 hours for cell isolation or PFA fixation.

Primary Human Mast Cell Lines

Peripheral blood mononuclear cells (PBMCs) were obtained from buffy coats (Etablissement Français du Sang). $CD34^+$ precursors cells were isolated from PBMCs (EasySep™ Human CD34 Positive Selection Kit, STEMCELL Technologies). $CD34^+$ cells were grown under serum-free conditions using StemSpan™ medium (STEMCELL Technologies) supplemented with recombinant human IL-6 (50 $ng.mL^{-1}$; Peprotech), human IL-3 (10 $ng.mL^{-1}$; Peprotech) and 3% supernatant of CHO transfectants secreting murine SCF (a gift from Dr. P. Dubreuil, Marseille, France, 3% correspond to ~50 $ng.mL^{-1}$ SCF) for one week. Cells were grown in IMDM Glutamax I, sodium pyruvate, 2-mercaptoethanol, 0.5% BSA, Insulin-transferrin selenium (all from Invitrogen), ciprofloxacin (10 $\mu g.mL^{-1}$; Sigma Aldrich), IL-6 (50 $ng.mL^{-1}$) and 3% supernatant of CHO transfectants secreting murine SCF for 8 weeks and tested both phenotypically ($Tryptase^+$, $CD117^+$, $Fc\varepsilon RI^+$) and functionally (β-hexosaminidase release in response to FcεRI crosslinking) before use in experiments. Only primary cell lines showing more than 95% $CD117^+/Fc\varepsilon RI^+$ cells were used for experiments.

Flow Cytometry

Cells from whole skin were dissociated into single-cell suspension by combining mechanical dissociation and enzymatic digestion. Briefly, the biopsies were washed in two successive PBS bathes, cut into 4 pieces and enzymatically digested by using the whole skin dissociation kit from Miltenyi biotec without enzyme P for 5 hours at 37°C under agitation (500 rpm). 500µL of cold RPMI 10% SCF were added to the samples and mechanical dissociation was achieved by using the BD™ Medimachine System (Becton-Dickinson). We optimized the tissue disaggregation in our experimental settings as follows: the 4 pieces were next placed into a disposable disaggregator Medicon™ with 50 µm separator mesh in 1 mL of ice-cold RPMI 10% SCF and processed in the Medimachine System by using a disaggregation time of 40 sec. The cell suspension was recovered from the Medicon unit with a 5-mL disposable syringe (the chamber was rinsed twice to increase yield) and was filtered (70 µm Filcon™ disposable filter device) and washed twice with RPMI 10% FCS. Cells were next split into three Eppendorf tubes and used for flow cytometry.

Antibodies were mixed according to the 2 multicolor flow cytometry panels (P1 and P2) at the concentration advised by the manufacturers in PBS 10% human serum (**Supplementary Figure 1** and **Table S1**) plus viability dye (Fixable viability dye-eFluor 506, eBiosciences). Cells were stained for 30 minutes at 4°C (with P1, P2 Ab mixes or PBS) washed twice in PBS/EDTA and acquired using BD LSR fortessa, flow rate calibration method was used to calculate absolute cell numbers. Data were analyzed using FlowJo software (V10, Tree Star).

Biopsies - Immunofluorescence – Confocal Microscopy

Biopsies for microscopy analysis were washed twice in PBS and fixed in PBS 4% PFA overnight at 4°C. The biopsies were washed for 5 min in a first bath of PBS and then for 24h in a second bath of PBS at 4°C and next bathed in PBS 30% sucrose for 48h at 4°C. Biopsies were next rinsed in two successive bathes of PBS for 2 hours and embedded in OCT™-Compound (Optimal Cuting Temperature-Compound; Tissu-Tek® Sakura), frozen and stored at -80°C until use. Biopsies were cut into 30 or 40 µm sections with a cryostat (Microm HM550 from Thermo Scientific) and mounted on adhesive glass slides and stored at -80°C until further use.

Frozen tissue sections were incubated for 10 minutes in PBS at 20°C and processed for antigen retrieval in HIER-EDTA pH 9.0 buffer (Zytomed Systems) at 90°C for 15 minutes. They were rinsed in PBS and blocked with PBS 20% human serum 0.3% saponin and next incubated with primary Abs diluted in PBS 20% human serum 0.3% saponin (**Supplementary Table S1**) for 16 hours at 4°C in a humidified chamber. They were next washed three times for 10 min and incubated with secondary Alexa Fluor-conjugated Abs (Invitrogen) for 2 hours at room temperature. Serial control sections were stained with the secondary Alexa Fluor-conjugated Abs alone (**Supplementary Figure 11**). After 3 washes of 10 minutes, nuclei were stained with DAPI for 5 minutes at 20°C. Images were acquired using Zeiss LSM 710 or LSM 780 confocal microscope (Zeiss, Oberkochen, Germany) and Zen Black software with a 40X/1.4 Oil Plan-Apochromatic objective. Control sections were used to set proper PMT (photomultiplier tube) gain, offset and collecting range.

Principal Component Analysis (PCA) and Data Clustering

We performed hierarchical clustering on flow cytometry data (numbers of the different cell population identified and percentages of Th cell subsets measured for the 3 stages of acne). Data were scaled and clustered, heatmap was obtained using heatmap.2 function of the gplots R package (complete linkage clustering using a Euclidean distance measure). PCA was next applied on these flow cytometry data to reduce the dimensionality (using the FactoMineR R package). The individuals' graph showed the distance between observations in the PC1 vs PC2 scatter plot and the variables' graph (correlation circle) showed the correlation among variables.

Mast Cell-CD4$^+$ T Cell Cocultures

2.10^5 CD4$^+$ effector/memory T cells (isolated from healthy donor PBMCs by negative selection using EasySep™ Human Memory CD4 T Cell Enrichment Kit, Stemcell) were incubated with 2.10^5 primary human mast cells (cell line established from a different donor) with or without anti-CD3/CD28-coated beads (Dynabeads™, Gibco) at a T cell:bead ratio of 10:1 in RPMI 10% FCS supplemented with 20 ng.mL^{-1} SCF. For RT-qPCR experiments, cells were harvested after 4, 24 or 48h incubation, stained with anti-CD117-PECy7 mAb (5 µg.mL^{-1}) and viability dye and sorted by a FACSMelody™ cell sorter (BD biosciences). In parallel experiments, Transwell inserts with polycarbonate 12 mm membrane diameter and 0.4µm pores were used to separate the cells in the co-culture (mast cells on top and CD4$^+$ T cell in the bottom). For immunofluorescence experiments, cells were transferred on poly-L-lysine-coated slides after 48h coculture.

Mast Cell-CD4$^+$ T Cell Cocultures - Immunofluorescence – Confocal Microscopy

After 48h coculture, cells were transferred on poly-L-lysine-coated slides and then fixed with 4% paraformaldehyde in PBS. Cells were first permeabilized and blocked in 10% normal human serum in PBS containing 0.3% saponin. Cells were stained with the following primary antibodies in PBS containing 1% BSA, 0.3% saponin for 2 hours at room temperature: anti-CD4, anti-IL-17A and anti-tryptase Abs (**Supplementary Table S1**). After washing, matched secondary antibodies (Alexa Fluor-conjugated donkey Abs, Invitrogen) were applied in PBS containing 1% BSA, 0.3% saponin for 45 min at RT. Control slides stained with secondary Abs alone were also performed. After 3 washes of 5 minutes, nuclei were stained with DAPI for 5 minutes at 20°C. The samples were mounted and examined using a Zeiss LSM 780 confocal microscope with a 63x Plan-Apochromat objective (1.4 oil). Control slides were used to set proper PMT (photomultiplier tube) gain, offset and collecting range. Scoring of the slides was performed in a blinded fashion by evaluating for each condition at least 200 mast cells in randomly selected fields from 3 independent experiments.

Real-Time Quantitative PCR

Total RNA was extracted from hMCs by using the phenol-chloroform method. IL-17A gene expression levels were measured by quantitative RT-PCR with Power SYBR Green technology (Applied Biosystems). Probes were obtained from Applied Biosystems as Assays-on-Demand™ Gene Expression Assays (glyceraldehyde-3-phosphate dehydrogenase GAPDH: Hs02758991_g1, IL-17A: HS 00174383_m1. Changes in relative gene expression were calculated using the $2^{-\Delta\Delta CT}$ method with normalization to GAPDH mRNA. All reactions were performed in three independent assays with three technical replicates.

Statistics

GraphPad Prism software (V.9; GraphPad Software, La Jolla, CA, USA) and R 4.0.3 were used for statistical analysis (stats package). Differences between groups were analyzed using one-way ANOVA (Dunnett's Multiple Comparison Test) or Friedman test with Dunn's *post hoc* test. Principal component Analysis (PCA) was applied on flow cytometry data (variables gathered in the heatmap **Figure 3A**) with the FactoMineR R package.

RESULTS

Immune Cell Landscape of the Early Stages of Acne

To quantify the immune infiltrate of the first stage of acneic lesion development and provide a detailed cartography of the spatial relationship between immune cell populations, we used both flow cytometry and microscopy approaches to study skin biopsies from a cohort of 15 young adults presenting with mild to moderate acne on the back (**Supplementary Figures 1A, B**). We focused our study on the early stages of pathology by collecting 3 types of skin biopsies: uninvolved (UI, i.e. skin without lesion in acne patient) skin, closed comedone (CC) and papule (PA) for each patient (**Supplementary Figures 1A, C**). We developed a protocol for cell dissociation from skin biopsies that maximizes viable immune cell recovery (notably macrophages and mast cells that tend to be attached to the extracellular matrix) and minimizes cell surface marker digestion during tissue preparation. We devised two surface maker panels in order to analyze the main leukocyte populations by multicolor flow cytometry (**Supplementary Figure 1**). The first panel was designed to identify lymphocytes and mast cells (**Supplementary Figure 2**). The second panel was designed to identify the monocyte/dendritic cell lineage populations and neutrophils (**Supplementary Figure 3**). Frequencies and composition of the cell populations identified by flow cytometry are presented in **Figure 1**. We showed an important population of $CD4^+$ T cells, present in UI skin, which increased as the lesion evolved. Cellularity increased significantly at the CC stage and continued increasing at the PA stage for all cell types except mast cells, whose cellularity peaked at the CC stage (**Supplementary Figure 4**). Of note, mast cells accounted for an important population of skin immune cells (13.0 ± 2.8% of $CD45^+$ cells), similar to the proportion of macrophages and resident dendritic cells in UI skin (**Figures 1A–C**). We observed that some cells such as neutrophils, monocytes and iDCs were scarce at the CC stage and started to be recruited at the PA stage. A massive infiltration of cells classically known to invade tissues early in the inflammatory process (namely neutrophils, monocytes, iDCs and B cells) was also observed at the PA stage (**Supplementary Figure 4**).

We investigated the activation status of the identified professional antigen presenting cells (APCs) by measuring CD40 and CD86 cell surface expression (**Supplementary Figure 5**). Because CD86 was expressed by virtually all APCs analyzed, we measured CD86 expression level (CD86 gMFI fold increase over control, **Supplementary Figures 5A, B**). We observed that among skin resident APCs, macrophages, cDC2s and $CD14^+$ DCs showed high CD86 expression level in UI skin. This expression level remained unchanged in macrophages from CC and PA biopsies while it increased from CC through PA stage in cDC2s. CD40 expression analysis showed a similar pattern (**Supplementary Figures 5C, D**). We further analyzed the mast cells that constitute an important sentinel cell population (**Figure 1**) and observed that the high affinity receptor for IgE, FcεRI, was upregulated through all of the acne stages studied (**Figures 2A, B**). Moreover, CD69 [an activation marker of mast cells (20, 21)] was strongly expressed in all the analyzed acne stages and its expression peaked at the CC stage, indicating that mast cells are activated very early in the acne process (**Figure 2C**).

Because Th17 and Th1 cells have been described as key players in acne, we aimed to identify these subsets by flow cytometry. To cope with the constraints imposed by the limited size of the biopsies, we opted for CD161 and CXCR3 markers to identify Th17 (22) and Th1 populations respectively (CCR6 was not used because it was degraded on the cell surface by the enzymatic digestion step). CD69 was also used as a marker of Ag-experienced skin resident T cells (14, 23, 24). $CD4^+$ conventional T cell analysis showed that an important proportion of $CD161^+$ cells was found in the skin (**Figures 2D, E**). It is worth noting that the majority of $CD161^+$ Th cells co-expressed CXCR3 in the UI and CC stages. $CXCR3^+$ $CD161^-$ Th cells represented the main Th cell population. All these population exhibited a dramatic increase at the CC stage and kept increasing at the PA stage (**Figure 2F**). The vast majority of $CD4^+$ Tconv cells, either $CD161^+$ or $CXCR3^+$, expressed CD69 in the UI and CC stages (**Figures 2G, H**). The percentage of $CD69^+$ Tconv cells decreased markedly at the PA stage. $CD69^+$ Th cell number peaked at the CC stage. Taken together, these results indicate that $CD161^+$ and $CXCR3^+$ Th cells dominate in acne skin and that these cells reside in UI skin as $CD69^+$ T cells. An important T cell infiltrate, mainly constituted of $CD69^-$ T cells, is observed as early as the CC stage.

Unsupervised Analysis of the Immune Cells Involved in CC and PA Stages of Acne

We next carried out an unsupervised analysis of the dataset obtained by flow cytometry. We included in the analysis the absolute cell numbers of the identified populations (**Figure 1**) and data concerning $CD4^+$ Tconv and $CD8^+$ T cells (**Figure 2**) as input variables. The heatmap (**Figure 3A**) summarizes these data

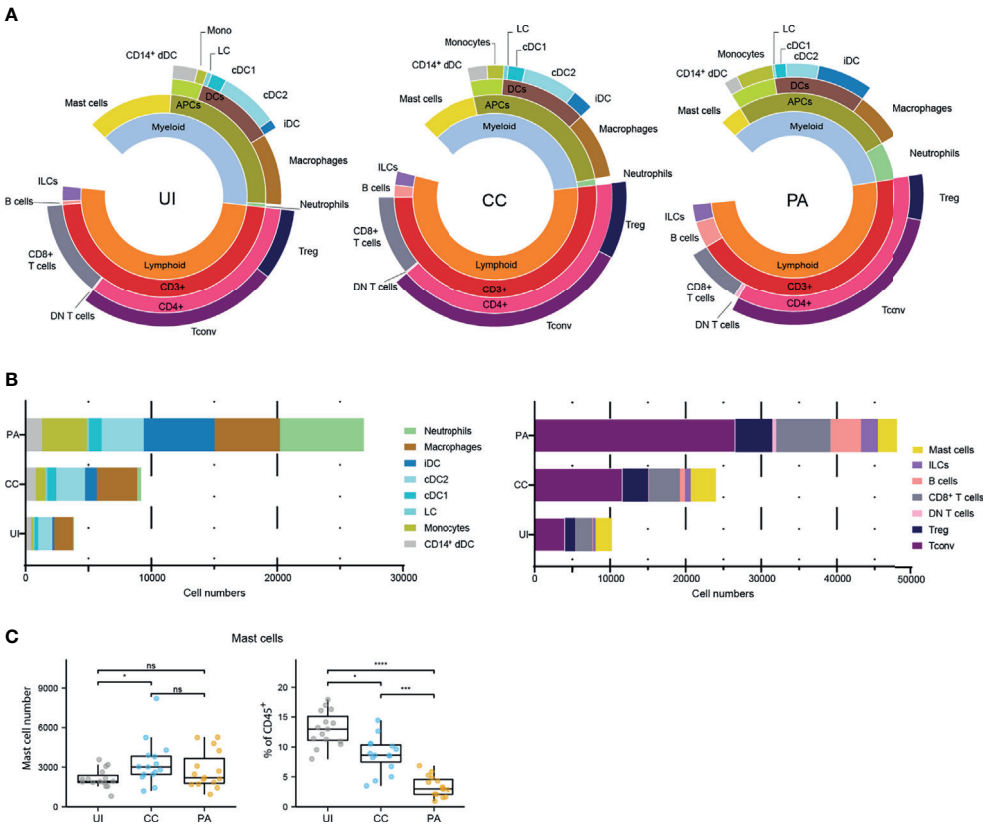

FIGURE 1 | Immune landscape of the early stages of acne. **(A)** Sunburst representation of the distributions and frequencies of the various cell subsets identified in the 3 stages. Results are expressed as percentages (means) of CD45$^+$ cells. **(B)** Stacked bar graph representing the average number of the major immune cell populations identified with the two flow cytometry panels. **(C)** Data for mast cell number and percentages of CD45$^+$ cells. Friedman test and Dunn's *post hoc* tests *p < 0.05; ***p < 0.001; ****p < 0.0001; ns, not significant. The other cell number evolution between the 3 stages are provided **Supplementary Figure 4**.

and presents a hierarchical clustering based on their correlation, making conspicuous the grouping of some variables (see colors in the dendrogram). The first group (blue color in **Figure 3A**) consists of blood leukocytes (neutrophils, monocytes, ILCs and B cells) whose number increased at the CC stage and peaked at the PA stage. These cells are known to be recruited during the inflammatory process or to differentiate after blood precursor recruitment. They participate in the local inflammatory response and contribute to the exacerbation of inflammation. Another group (red color in **Figure 3A**) consists of skin resident leukocytes, whose absolute number increases substantially at the CC stage (CD14$^+$ dDCs, macrophages, cDC2s, cDC1s and T cells). Two other skin resident cells (LCs and mast cells, color green in **Figure 3A**) increased at the CC stage and stabilized at the PA stage.

Principal component analysis (PCA) showed that the expression profiles of the 3 acne stages are distinguishable (**Figure 3B**). The first dimension clearly distinguishes the different stages, with the PA stage showing the highest values. Analysis of the loadings plot showed that the number of CD8$^+$ T cells, Tconv cells, monocytes, iDCs, and neutrophils (**Figure 3C**) contributed strongly to this dimension. It indicates that the first dimension is associated with inflammatory cell infiltration. On the contrary, UI biopsies are gathered on the left of this axis following the direction of CD69$^+$ T cells. CD69$^+$ T cells and low infiltrate characterize the UI skin. Another group of variables contributed to the second PCA dimension (notably Th17, Th1.17, mast cells and CD14$^+$ dDCs). The CC biopsies exhibited globally higher values in this second dimension, indicating that these populations are defining features of the CC stage. Moreover, their associated vectors are adjacent in the correlation circle, indicating that these variables are positively correlated (**Figure 3C**).

Microscopy Analysis of IL-17-Producing Mast Cells in the Early Stages of Acne

Because we identified cDC2 activation during the early stages of acne and because these cells have been shown to promote type 3 responses (25), our next approach was to create a cartography of cDC2 and IL-17$^+$ CD4$^+$ T cells using confocal microscopy. We employed the CD1c marker (26, 27) to identify cDC2s.

To generate a global view of each biopsy, tile scans of 30-40 sequential z-planes were acquired, creating a 3D mosaic of adjacent image stacks. In the CC and PA stages, we observed a perifollicular accumulation of CD4$^+$ T lymphocytes and CD1c$^+$

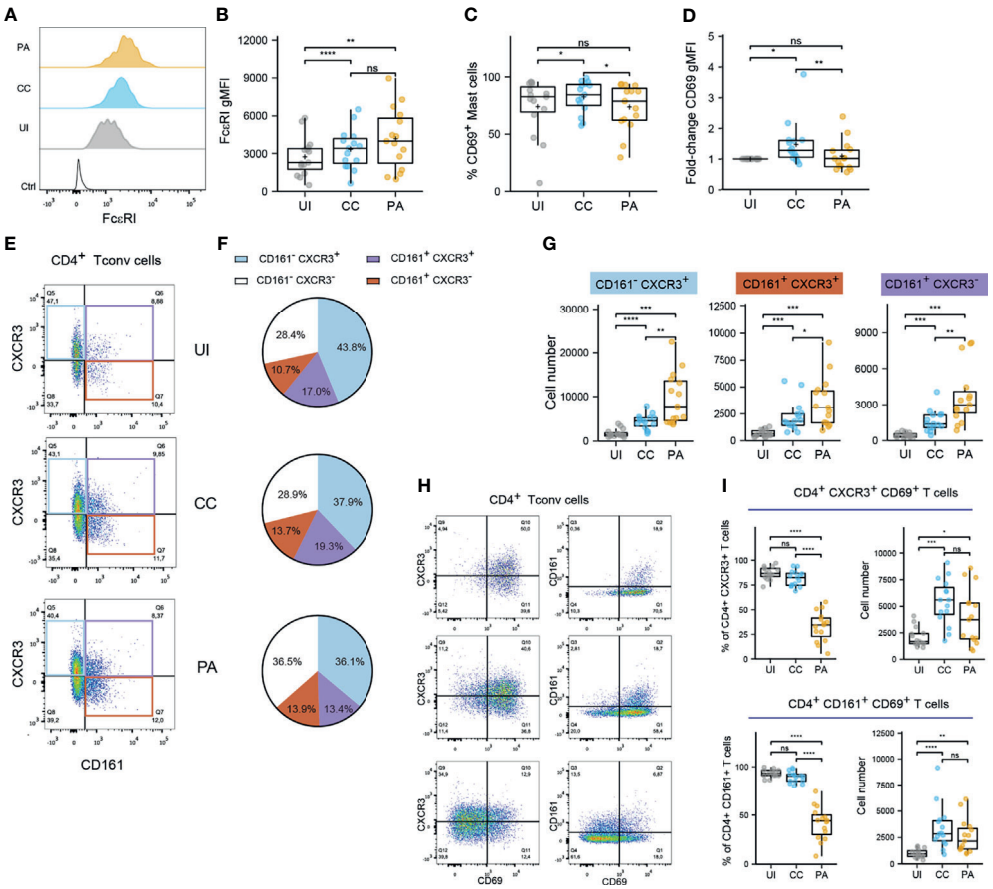

FIGURE 2 | Mast cells and CD4$^+$ T cells exhibit activated in the early stages of acne. **(A, B)** FcεRI expression by mast cells. Typical histograms **(B)** and pooled data as FcεRI gMFI values from the 15 patients. **(C, D)** CD69 expression by mast cells. % CD69$^+$ mast cell **(C)** and CD69 gMFI fold-change over UI skin **(D)**. Points represent the individual values for the 15 patients. Box and whiskers plots in the style of Tukey. *p < 0.05; **p < 0.01; ns, not significant (one-way ANOVA and Fisher's least significant difference *post hoc* test). **(E)** Representative dotplot of CD161 and CXCR3 expression within CD4$^+$ Tconv cells (CC stage) and **(F)** average percentages of CD161/CXCR3 populations within CD4$^+$ Tconv cells (15 patients). **(G)** Number of indicated CD161/CXCR3 CD4$^+$ Tconv cell populations. **(H)** Representative dotplot of CD69, CD161 and CXCR3 expression within CD4$^+$ Tconv cells (CC stage). **(I)** Percentage and number of CD69$^+$ cells among CXCR3$^+$ or CD161$^+$ CD4$^+$ Tconv cells. Box and whiskers plot in the style of Tukey. Each point represents a patient. Friedman tests were carried out to compare groups and, if significant, were followed by Dunn's *post hoc* tests *p < 0.05; **p < 0.01; ***p < 0.001; ****p < 0.0001; ns, not significant.

cells (**Supplementary Figures 6A**, **7A**, areas highlighted in yellow) as well as clusters of perivascular immune cells enriched in CD4$^+$ T cells and cDC2s along the rete subpapillare. In some biopsies, clusters of CD4$^+$ T cells could be observed deeper in the dermis. CD1c staining revealed a lining of cDC2s just beneath the dermo-epidermis junction in the papillary dermis (**Supplementary Figures 6A**, **7A**). It was not possible to compare the cell infiltrates between CC and PA stages because cellularity depended upon the area sampled by the slicing procedure. Nevertheless, perifollicular accumulation of CD4$^+$ T cells appeared larger in some PA biopsies when compared to their CC counterparts, which was combined with a thickening of the epidermis at the PA stage (**Supplementary Figure 6E**). We observed that the majority of CD1c$^+$ cells resided either in the CD4$^+$ T cell enriched areas or just beneath the dermo-epidermal junction (**Supplementary Figures 6A, B** and **7A, B**). Unexpectedly, IL-17 staining revealed that CD4$^+$ T cells represented only a minor fraction of IL-17$^+$ cells, but non-CD4$^+$ cells that stained positive for IL-17 appeared to be preferentially located in CD4$^+$ T cell clusters. IL-17 staining was often punctate and covered a large part of the cell cytoplasm (**Supplementary Figures 6C, D** and **7C, D**).

These results prompted us to identify the other cells that produced IL-17. We labelled neutrophils with myeloperoxidase (MPO), macrophages with FXIIIA, mast cells with tryptase and the whole T cell population with CD3 staining. Using triple staining immunofluorescence (tryptase, CD3 and IL-17), we observed an abundance of tryptase/IL-17 double positive cells in CC biopsy sections, indicating that mast cells stained positive for IL-17 (**Figures 4A, B**). Macrophages did not stain positive for IL-17 (**Supplementary Figure 8**). We observed some IL-17$^+$ MPO$^+$ cells in PA biopsies infiltrated by neutrophils but they were not the main IL-17$^+$ cell population (**Supplementary Figure 9**). We next quantified the CD3$^+$/IL-17$^+$ cells or tryptase$^+$/IL-17$^+$ cells

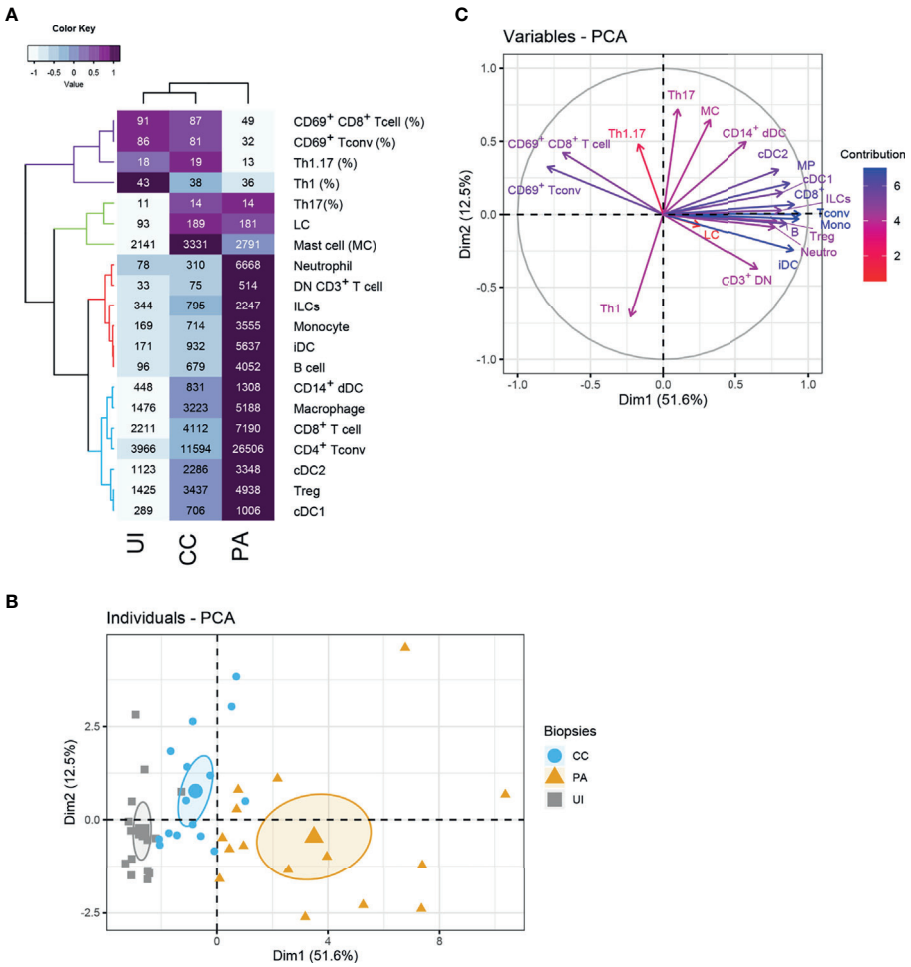

FIGURE 3 | Unsupervised analysis of the skin immune profiles of UI, CC and PA biopsies. **(A)** Heatmap depicting flow cytometry parameters calculated for UI, CC and PA biopsies (n=15 patients). The mean of each indicated flow cytometry parameter (showed in the cells) was scaled, centered, clustered hierarchically with complete linkage and Euclidean distance measure and visualized in the heatmap using the function heatmap.2 of the gplots R package. Principal component analysis (PCA) was performed with flow cytometry variables shown in the heatmap. **(B)** Individuals' PCA. Each dot represents one patient, color was attributed according to the acne stage. The bigger dot shows the group barycenter. The confidence interval of the mean (0.95%) is represented by ellipses. **(C)** PCA variable correlation plot. Variable contribution is shown by color code. Th1: CD161$^-$ CXCR3$^+$ T conv cells, Th17: CD161$^+$ CXCR3$^-$ T conv cells; Th1.17: CD161$^+$ CXCR3$^+$ T conv cells; CD3$^+$ DN T cells: CD3$^+$ CD4$^-$ CD8$^-$ cells.

in MC and PA biopsies in 4 patients (**Figure 4C**). Because we have previously shown that mast cells can cooperate with antigen-experienced T cells (21, 28), we also analyzed whether the IL-17 positive or negative mast cells were inside or outside the T cell clusters (perifollicular or perivascular). The contingency tables obtained from the quantification of 4 CC and 4 PA biopsies from 4 different patients indicated that mast cells inside the T cell clusters were clearly more prone to produce IL-17 than their counterparts outside T cell clusters (**Figure 4D**).

Activated Memory CD4$^+$ T Cells Induced IL-17 Production by Mast Cells

We next investigated the stimuli able to induce IL-17 production by mast cells using primary mast cell lines derived from peripheral blood CD34$^+$ precursors (hMCs). We first stimulated hMCs with classical activating stimuli (IgE/anti-IgE, substance P, C5a, TLR2 and TLR4 ligands with or without priming with AhR ligands) or combinations of cytokines known to promote IL-17 production in T cells (such as IL-1β, IL-23 and IL-6) but we did not detect any IL-17 production in the conditions tested (data not shown).

The relationship observed between IL-17 production by mast cells and their localization in T cell rich areas prompted us to test whether activated CD4$^+$ T cells might induce IL-17 production by hMCs. Moreover, the observation that some IL-17$^+$ mast cells located in T cell rich areas were in close proximity to CD4$^+$ T cells reinforced this hypothesis (**Figure 5A**). We cocultured hMCs with *ex vivo* sorted effector/memory CD4$^+$ T cells stimulated with anti-CD3/CD28 coated beads. Because both

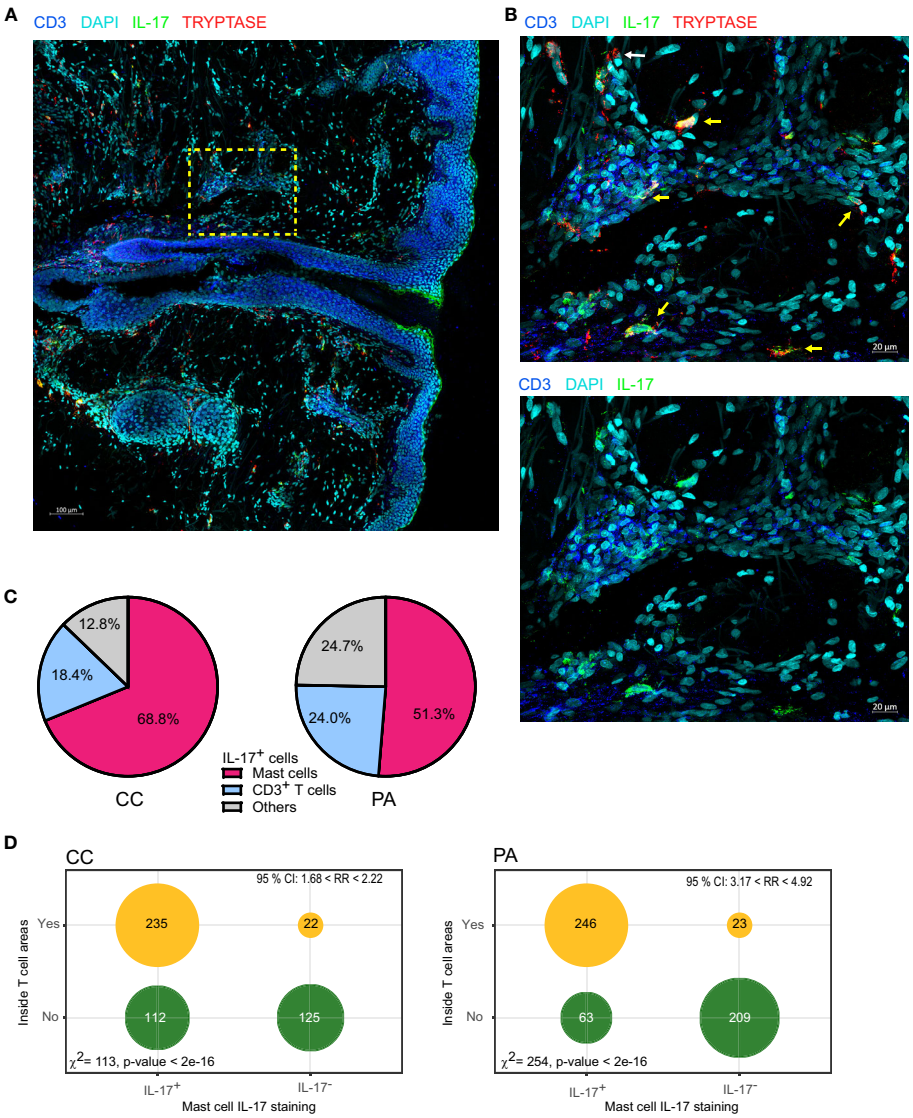

FIGURE 4 | Mast cells are the main cells staining IL-17$^+$ in the early stages of acne. **(A)** A representative image depicting IL-17, CD3 and tryptase staining (CC stage). **(B)** High-magnification image showing IL-17$^+$ mast cells (yellow arrows) near perifollicular area (bottom) and perivascular area (top); white arrow points IL-17$^-$ mast cell. **(C)** Image quantification of IL-17$^+$ cells among CD3$^+$ (T cells), Tryptase$^+$ (mast cells), pooled data from 4 patients either at CC or PA stage as indicated. **(D)** Tryptase$^+$ cells were classified according to IL-17 staining and to location (inside or outside T cell rich areas as depicted in **Supplementary Figure 2**), resulting contingency tables of counts are plotted (pooled data from 4 patients); χ^2 test for independence and relative risk are indicated.

CD4$^+$ T cells and mast cells could produce IL-17, we FACS-sorted mast cells after coculture and measured *IL-17A* mRNA by RTqPCR. IL-17A mRNA was induced after 4h coculture and increased up to 24 hours (**Figure 5B**). In parallel experiments, cell contact was blocked by physically separating the cells with Transwell inserts (0.4µm) and no IL-17A mRNA induction was observed (**Figure 5C**) indicating that cell-cell contacts are necessary for the activated CD4$^+$ T cell to drive IL-17A gene transcription in mast cells. Because hMC viability might be impacted after 48h coculture and impair their ability to produce cytokines, we analyzed the viability of the cells at the end of the coculture by FACS. We observed that hMC viability was higher than 95% under all the conditions tested, allowing us to rule out this hypothesis (**Supplementary Figure 10**). To analyze IL-17 expression at the protein level, we analyzed mast cell/CD4$^+$ T cell cocultures by confocal microscopy following immunofluorescence staining of intracellular IL-17 and tryptase to unambiguously identify mast cells (**Figure 5D**). Whilst less than 3% of mast cells were IL-17$^+$ following coculture with unstimulated CD4$^+$ T cells, more than half of them were IL-17$^+$ following coculture with anti-CD3/CD28-stimulated CD4$^+$ T cells. Collectively, these results indicated that mast cell interaction with activated memory/effector CD4$^+$ T cells promoted IL-17 production by mast cells.

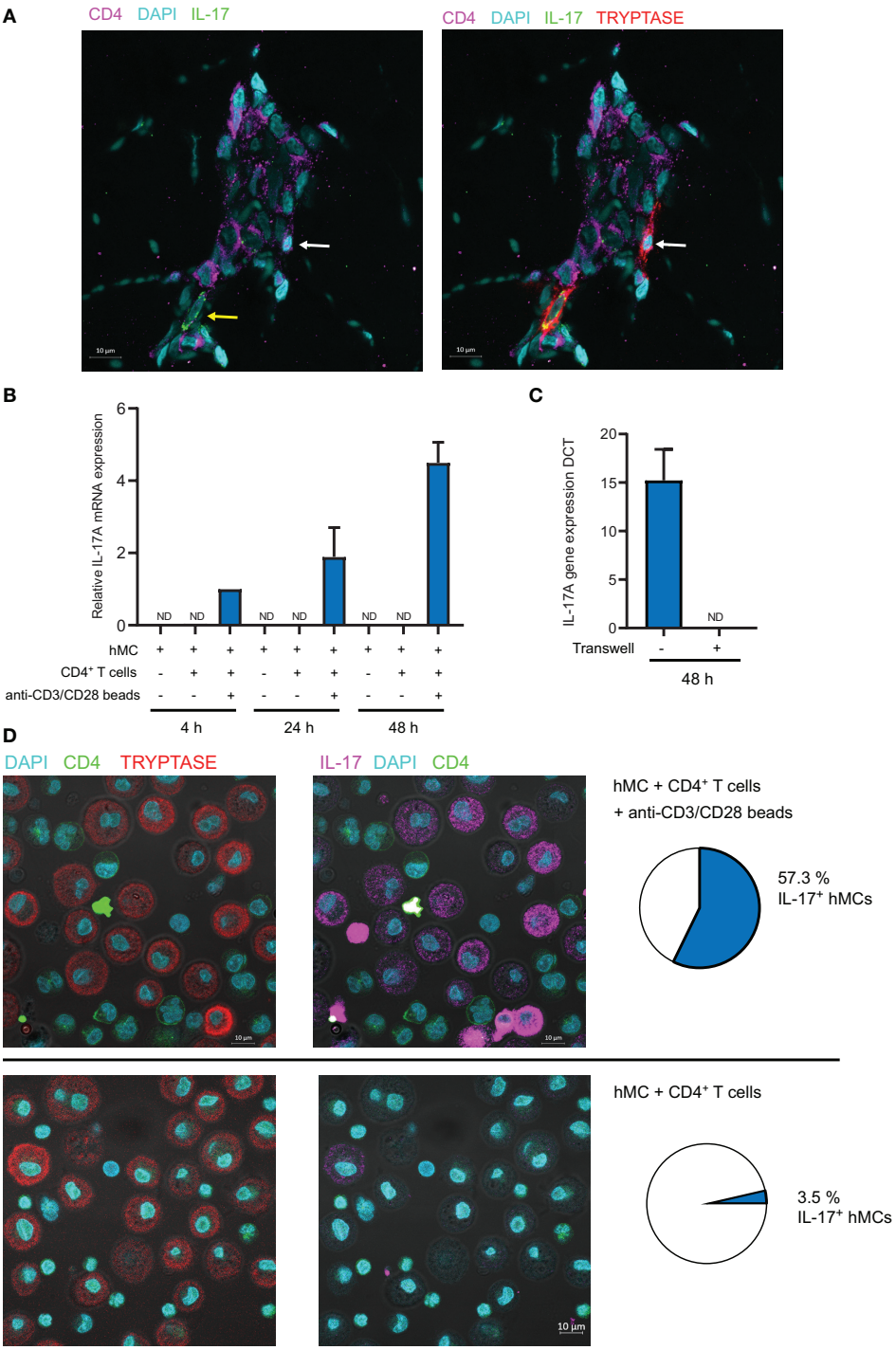

FIGURE 5 | Activated CD4$^+$ memory T cells induce IL-17A mRNA expression in mast cells in a contact-dependent manner. **(A)** Typical example of tryptase+ mast cell in contact with CD4+ T cell in CC biopsy. Yellow arrow shows IL-17$^+$ mast cell, White arrow shows IL-17$^-$ mast cell. **(B)** hMCs and memory CD4$^+$ T cells were cocultured (with or without anti-CD3/CD28 coated beads) for indicated time. hMCs were FACS sorted and IL-17A mRNA expression was quantified by RTqPCR. **(C)** hMCs and activated memory CD4$^+$ T cells with anti-CD3/CD28 coated beads were cocultured for 48h with or without the possibility to establish contacts (separation by a 0.4µm membrane in Transwell coculture systems). hMCs were FACS sorted and IL-17A mRNA expression was quantified by RTqPCR. Mean +/- SD from 3 independent experiments (hMCs from 3 different donors). **(D)** IL-17 and tryptase intracellular stainings in hMCs and memory CD4$^+$ T cells cocultured (with or without anti-CD3/CD28 coated beads) for 48h. Typical confocal images and quantification of IL-17$^+$ hMCs (n>200) representative of 3 independent experiments (3 different hMC/CD4$^+$ T cell pairs). ND, not detected.

DISCUSSION

In this study, we employed both flow cytometry- and microscopy-based approaches to delineate the immune landscape of the early stages of acne. Our quantitative analysis corroborated the view that significant cellular changes occur early in acne lesion development, before clinical symptoms appear.

Our unsupervised analysis clearly demonstrated that specific cell populations cluster together and that different clusters dominate at different stages of lesion development. The evolution of these populations is a defining feature of acne immunopathogenesis. Mast cells appeared as pioneer cells in the acne immune response followed by the group of resident APCs ($CD14^+$ dDCs, macrophages, cDC2s, cDC1s) and resident T cells. These three groups of cells could be suspected to play a role in the initiation of the acne process. The hypothesis of an immune response burden in uninvolved skin in patients with acne is reinforced by the fact that we observed a high percentage of activated mast cells and macrophages (according to CD86 and CD40 expression) in UI biopsies. This point is reinforced by CD69 expression on the mast cell surface in UI skin as well as during the CC and PA stages, suggesting that these cells are implicated very early in acne. It would have been interesting to analyze UI skin by microscopy but the local ethic committee refused the second biopsy of UI skin.

To analyze the T cell response specifically, we devised a flow cytometry panel to identify $CD8^+$ T cells, $CD4^+$ Tconv and Treg cells. Because repeated exposure to commensal microorganisms (notably *C. acnes*) is expected to occur in acne and because previous reports showed the importance of the Th1 and Th17 axes in acne (18, 19, 29), we chose to target Th1, Th17 and TRM cells in our analysis. We employed CXCR3 to identify Th1 cells (30–32) and CD161 to identify IL-17 producing T cells (33, 34). Although CXCR3 and CD161 are often found in Th1 and Th17 cell subsets respectively, they do not strictly define them. Nevertheless, these markers provided a reasonable approximation for our analysis of $CD4^+$ Tconv cells. The presence of a substantial contingent of Th17 cells ($CD4^+CD161^+$ Tconv cells) in the skin at steady state is not surprising because these cells are known to participate in immune surveillance of barrier organs. $CD4^+CD161^+$ Tconv cells are expected to belong to the Th17 subset, but CD161 expression is not synonymous with IL-17 production because these cells need to engage their TCR to produce cytokines. Our work quantifies for the first time $CD161^+$ T cells in acne and we note a clear increase of Th17 cell number in the CC stage, indicating an early involvement of this subset in acne pathogenesis. In line with previous reports (18, 19, 29, 35), we show that Th17 cell numbers are increased in acne and we support the notion that these cells are recruited and/or proliferate during CC formation while they are already present in UI skin of patients with acne. Moreover, the combined analysis of CXCR3 and CD161 showed the presence of cells expressing both markers (about 15% of Tconv cells) that are reminiscent of pathogenic Th17.1 cells (36, 37), that produce both IL-17 and IFN-γ, previously described in autoimmunity or autoinflammation (38).

The analysis of CD69 expression by $CD4^+$ and $CD8^+$ Tconv cells showed that the large majority of these cells were $CD69^+$ in UI skin. CD69 is a classical early activation marker *in vitro*. It also appears to be associated with tissue retention *in vivo* thanks to its capacity to counteract S1P-mediated egress and is expressed by memory T cell subsets that are retained in the periphery (23, 39). CD69 is expressed notably by tissue-resident memory T cells (TRM) (14, 40–44). TRM are now under intensive investigation and CD69 expression appears to be a hallmark of TRM cells. In line with previous reports, we observed that the percentage of $CD69^+$ $CD4^+$ or $CD8^+$ T cells was very high in UI skin biopsies (44, 45). It is likely that these cells in UI skin represent TRM cells that accumulated *via* repeated immune responses against skin commensal microorganisms in patients with acne. The fact that $CD69^+$ absolute cell number increased (for both $CD4^+$ and $CD8^+$ T cells) at the CC stage and plateaued at the PA stage (a non-significant slight decrease was measured) suggests that these TRM cells might be involved and proliferate in the very early steps of acne pathogenesis. At the PA stage, an important recruitment of $CD69^-$ effector T cells and/or possibly a loss of CD69 by some proliferating TRM cells is observed. This scenario is compatible with what was observed by Park et al., in skin challenged with *C. albicans* (46). It is tempting to speculate that locally activated commensal-specific TRM cells (in cooperation with local APC such as cDC2s, macrophages or $CD14^+$ dDCs) drive the progression of the acne inflammatory process. These early activated cells are next joined at the PA stage by infiltrating of proliferating effector T cells ($CD4^+$, $CD8^+$ and γδ T cells that certainly represent the majority of the $CD3^+$ DN cells identified by flow cytometry) that can produce inflammatory cytokines such as IFN-γ and TNF.

The early involvement of T cell responses prompted us to investigate by microscopy the location of IL-17 producing $CD4^+$ T cells in relation with cDC2s. We focused on cDC2s because they were expected to drive Th17 responses (47) and because we observed that they were activated in CC biopsies. In agreement with Natsuaki et al. (48, 49), we observed large perivascular clusters of DC and $CD4^+$ T cells in CC as well as PA biopsies. Nevertheless, we were surprised to observe that $CD4^+$ T cells were not the main $IL\text{-}17^+$ population and that instead, IL-17 appeared to be produced by mast cells, notably in CC biopsies. It appears that in acne, as was reported in psoriasis, T cells are not the main $IL\text{-}17^+$ population (50, 51).

We found that mast cell number peaked at the CC stage and represented about 10-12% of $CD45^+$ cells. This observation might be explained by an increase of stem cell factor (SCF) production by keratinocytes, since alteration of the microbiota was reported to increase the mast cell population indirectly by acting on SCF production by keratinocytes (52, 53). IL-17 is not a typical mast cell cytokine but several studies reported $IL\text{-}17^+$ mast cells in different pathophysiological conditions (50, 54–60). However, no mechanism underlying IL-17 production by mast cells in these situations was reported. Here, we showed that activated Th cells license mast cells to activate IL-17A transcription *via* cell-cell contacts. This indicates that mast cells are able to produce their own IL-17 following cell-cell cooperation with $CD4^+$ T cells. This result echoes our previous work showing that Th cell-mast cell cooperation fosters mast cell degranulation upon IgE/Ag stimulation (21). Nevertheless, if triggering of MCs *via* IgE/Ag in the context of acne is very unlikely, several other stimuli can be

envisaged (11, 12). The fact that neither classical MC stimuli nor Th cell cytokines did not induce IL-17 production suggests that IL-17 production by MCs is tightly regulated and probably relies on a combination of membrane and soluble Th cell ligands.

Taken together, these results show for the first time that mast cells are an effector cell of the early immune response in acne, which is controlled by the Th cell response. We can infer that mast cells serve as early innate effector cell (notably as an early IL-17 source) in acne pathogenesis, driven by the nascent Th17 and Th1.17 responses (possibly due to the reactivation of TRM cells). In later stages of the pathology, neutrophils take over and amplify the IL-17 production. This study paves the road for further investigations to evaluate the role of mast cells in acne beyond IL-17 production. Moreover, it identifies mast cells as new strategic therapeutic targets in acne.

DATA AVAILABILITY STATEMENT

The original contributions presented in the study are included in the article/**Supplementary Material**. Further inquiries can be directed to the corresponding author.

ETHICS STATEMENT

The studies involving human participants were reviewed and approved by CCP Sud-ouest et Outremer III. The patients/participants provided their written informed consent to participate in this study.

AUTHOR CONTRIBUTIONS

Conceptualization: DR and EE. Supervision: EE. Formal analysis: EE. Investigation: YE, EL, LB, and TN. Visualization: EE and EL. Validation LG and EE. Writing – Original Draft Preparation: EE. Writing - Review and Editing: BM. All authors contributed to the article and approved the submitted version.

FUNDING

This research was supported by INSERM (Institut national de la santé et de la recherche médicale) and by Pierre Fabre Dermo-Cosmétique (PFDC). The funder was not involved in the study design, collection, analysis, interpretation of data, the writing of this article or the decision to submit it for publication.

ACKNOWLEDGMENTS

We thank the flow cytometry and imaging core facilities of the INSERM UMR 1043, CPTP and of the INSERM UMR 1037, CRCT, Toulouse, France.

SUPPLEMENTARY MATERIAL

The Supplementary Material for this article can be found online at: https://www.frontiersin.org/articles/10.3389/fimmu.2021.740540/full#supplementary-material

REFERENCES

1. Tuchayi SM, Makrantonaki E, Ganceviciene R, Dessinioti C, Feldman SR, Zouboulis CC. Acne Vulgaris. *Nat Rev Dis Primers* (2015) 1(1):15029. doi: 10.1038/nrdp.2015.29
2. Saurat JH. Strategic Targets in Acne: The Comedone Switch in Question. *Dermatology* (2015) 231(2):105–11. doi: 10.1159/000382031
3. Cunliffe WJ, Holland DB, Jeremy A. Comedone Formation: Etiology, Clinical Presentation, and Treatment. *Clinics Dermatol* (2004) 22(5):367–74. doi: 10.1016/j.clindermatol.2004.03.011
4. Do TT, Zarkhin S, Orringer JS, Nemeth S, Hamilton T, Sachs D, et al. Computer-Assisted Alignment and Tracking of Acne Lesions Indicate That Most Inflammatory Lesions Arise From Comedones and De Novo. *J Am Acad Dermatol* (2008) 58(4):603–8. doi: 10.1016/j.jaad.2007.12.024
5. Norris JF, Cunliffe WJ. A Histological and Immunocytochemical Study of Early Acne Lesions. *Br J Dermatol* (1988) 118(5):651–9. doi: 10.1111/j.1365-2133.1988.tb02566.x
6. Layton AM, Morris C, Cunliffe WJ, Ingham E. Immunohistochemical Investigation of Evolving Inflammation in Lesions of Acne Vulgaris. *Exp Dermatol* (1998) 7(4):191–7. doi: 10.1111/j.1600-0625.1998.tb00323.x
7. Jeremy AHT, Holland DB, Roberts SG, Thomson KF, Cunliffe WJ. Inflammatory Events Are Involved in Acne Lesion Initiation. *J Invest Dermatol* (2003) 121(1):20–7. doi: 10.1046/j.1523-1747.2003.12321.x
8. Mouser PE, Baker BS, Seaton ED, Chu AC. Propionibacterium Acnes-Reactive T Helper-1 Cells in the Skin of Patients With Acne Vulgaris. *J Invest Dermatol* (2003) 121(5):1226–8. doi: 10.1046/j.1523-1747.2003.12550_6.x
9. Belkaid Y, Tamoutounour S. The Influence of Skin Microorganisms on Cutaneous Immunity. *Nat Rev Immunol* (2016) 16(6):353–66. doi: 10.1038/nri.2016.48
10. Kabashima K, Honda T, Ginhoux F, Egawa G. The Immunological Anatomy of the Skin. *Nat Rev Immunol* (2019) 19(1):19–30. doi: 10.1038/s41577-018-0084-5
11. Valent P, Akin C, Hartmann K, Nilsson G, Reiter A, Hermine O, et al. Mast Cells as a Unique Hematopoietic Lineage and Cell System: From Paul Ehrlich's Visions to Precision Medicine Concepts. *Theranostics* (2020) 10 (23):10743–68. doi: 10.7150/thno.46719
12. Siiskonen H, Harvima I. Mast Cells and Sensory Nerves Contribute to Neurogenic Inflammation and Pruritus in Chronic Skin Inflammation. *Front Cell Neurosci* (2019) 13:422(422). doi: 10.3389/fncel.2019.00422
13. Voss M, Kotrba J, Gaffal E, Katsoulis-Dimitriou K, Dudeck A. Mast Cells in the Skin: Defenders of Integrity or Offenders in Inflammation? *Int J Mol Sci* (2021) 22(9):4589. doi: 10.3390/ijms22094589
14. Watanabe R, Gehad A, Yang C, Scott LL, Teague JE, Schlapbach C, et al. Human Skin Is Protected by Four Functionally and Phenotypically Discrete Populations of Resident and Recirculating Memory T Cells. *Sci Transl Med* (2015) 7(279):279ra239. doi: 10.1126/scitranslmed.3010302
15. Annunziato F, Romagnani C, Romagnani S. The 3 Major Types of Innate and Adaptive Cell-Mediated Effector Immunity. *J Allergy Clin Immunol* (2015) 135(3):626–35. doi: 10.1016/j.jaci.2014.11.001
16. McGeachy MJ, Cua DJ, Gaffen SL. The IL-17 Family of Cytokines in Health and Disease. *Immunity* (2019) 50(4):892–906. doi: 10.1016/j.immuni.2019.03.021
17. Ebrahim AA, Mustafa AI, El-Abd AM. Serum Interleukin-17 as a Novel Biomarker in Patients With Acne Vulgaris. *J Cosmet Dermatol* (2019) 18 (6):1975–9. doi: 10.1111/jocd.12934
18. Agak GW, Qin M, Nobe J, Kim MH, Krutzik SR, Tristan GR, et al. Propionibacterium Acnes Induces an IL-17 Response in Acne Vulgaris That Is Regulated by Vitamin A and Vitamin D. *J Invest Dermatol* (2014) 134(2):366–73. doi: 10.1038/jid.2013.334

19. Kelhala HL, Palatsi R, Fyhrquist N, Lehtimaki S, Vayrynen JP, Kallioinen M, et al. IL-17/Th17 Pathway Is Activated in Acne Lesions. *PloS One* (2014) 9(8): e105238. doi: 10.1371/journal.pone.0105238
20. Jayapal M, Tay HK, Reghunathan R, Zhi L, Chow KK, Rauff M, et al. Genome-Wide Gene Expression Profiling of Human Mast Cells Stimulated by IgE or Fcεri-Aggregation Reveals a Complex Network of Genes Involved in Inflammatory Responses. *BMC Genomics* (2006) 7(1):210. doi: 10.1186/1471-2164-7-210
21. Gaudenzio N, Espagnolle N, Mars LT, Liblau R, Valitutti S, Espinosa E. Cell-Cell Cooperation at the T Helper Cell/Mast Cell Immunological Synapse. *Blood* (2009) 114(24):4979–88. doi: 10.1182/blood-2009-02-202648
22. Maggi L, Santarlasci V, Capone M, Peired A, Frosali F, Crome SQ, et al. CD161 Is a Marker of All Human IL-17-Producing T-Cell Subsets and Is Induced by RORC. *Eur J Immunol* (2010) 40(8):2174–81. doi: 10.1002/eji.200940257
23. Mackay LK, Braun A, Macleod BL, Collins N, Tebartz C, Bedoui S, et al. Cutting Edge: CD69 Interference With Sphingosine-1-Phosphate Receptor Function Regulates Peripheral T Cell Retention. *J Immunol* (2015) 194 (5):2059–63. doi: 10.4049/jimmunol.1402256
24. Mueller SN, Mackay LK. Tissue-Resident Memory T Cells: Local Specialists in Immune Defence. *Nat Rev Immunol* (2016) 16(2):79–89. doi: 10.1038/nri.2015.3
25. Schlitzer A, McGovern N, Teo P, Zelante T, Atarashi K, Low D, et al. IRF4 Transcription Factor-Dependent CD11b+ Dendritic Cells in Human and Mouse Control Mucosal IL-17 Cytokine Responses. *Immunity* (2013) 38 (5):970–83. doi: 10.1016/j.immuni.2013.04.011
26. Zaba LC, Fuentes-Duculan J, Steinman RM, Krueger JG, Lowes MA. Normal Human Dermis Contains Distinct Populations of CD11c+BDCA-1+ Dendritic Cells and CD163+FXIIIA+ Macrophages. *J Clin Invest* (2007) 117 (9):2517–25. doi: 10.1172/jci32282
27. Granot T, Senda T, Carpenter DJ, Matsuoka N, Weiner J, Gordon CL, et al. Dendritic Cells Display Subset and Tissue-Specific Maturation Dynamics Over Human Life. *Immunity* (2017) 46(3):504–15. doi: 10.1016/j.immuni.2017.02.019
28. Gaudenzio N, Laurent C, Valitutti S, Espinosa E. Human Mast Cells Drive Memory CD4+ T Cells Toward an Inflammatory IL-22+ Phenotype. *J Allergy Clin Immunol* (2013) 131(5):1400–7.e1411. doi: 10.1016/j.jaci.2013.01.029
29. Kistowska M, Meier B, Proust T, Feldmeyer L, Cozzio A, Kuendig T, et al. Propionibacterium Acnes Promotes Th17 and Th17/Th1 Responses in Acne Patients. *J Invest Dermatol* (2015) 135(1):110–8. doi: 10.1038/jid.2014.290
30. Langenkamp A, Nagata K, Murphy K, Wu L, Lanzavecchia A, Sallusto F. Kinetics and Expression Patterns of Chemokine Receptors in Human CD4+ T Lymphocytes Primed by Myeloid or Plasmacytoid Dendritic Cells. *Eur J Immunol* (2003) 33(2):474–82. doi: 10.1002/immu.200310023
31. Groom JR, Richmond J, Murooka TT, Sorensen EW, Sung JH, Bankert K, et al. CXCR3 Chemokine Receptor-Ligand Interactions in the Lymph Node Optimize CD4+ T Helper 1 Cell Differentiation. *Immunity* (2012) 37(6):1091–103. doi: 10.1016/j.immuni.2012.08.016
32. Brodie T, Brenna E, Sallusto F. OMIP-018: Chemokine Receptor Expression on Human T Helper Cells. *Cytometry A* (2013) 83A(6):530–2. doi: 10.1002/cyto.a.22278
33. Cosmi L, De Palma R, Santarlasci V, Maggi L, Capone M, Frosali F, et al. Human Interleukin 17-Producing Cells Originate From a CD161+CD4+ T Cell Precursor. *J Exp Med* (2008) 205(8):1903–16. doi: 10.1084/jem.20080397
34. Kleinschek MA, Boniface K, Sadekova S, Grein J, Murphy EE, Turner SP, et al. Circulating and Gut-Resident Human Th17 Cells Express CD161 and Promote Intestinal Inflammation. *J Exp Med* (2009) 206(3):525–34. doi: 10.1084/jem.20081712
35. Mashiko S, Bouguermouh S, Rubio M, Baba N, Bissonnette R, Sarfati M. Human Mast Cells Are Major IL-22 Producers in Patients With Psoriasis and Atopic Dermatitis. *J Allergy Clin Immunol* (2015) 136(2):351–9.e351. doi: 10.1016/j.jaci.2015.01.033
36. Annunziato F, Cosmi L, Santarlasci V, Maggi L, Liotta F, Mazzinghi B, et al. Phenotypic and Functional Features of Human Th17 Cells. *J Exp Med* (2007) 204(8):1849–61. doi: 10.1084/jem.20070663
37. Ramesh R, Kozhaya L, McKevitt K, Djuretic IM, Carlson TJ, Quintero MA, et al. Pro-Inflammatory Human Th17 Cells Selectively Express P-Glycoprotein and Are Refractory to Glucocorticoids. *J Exp Med* (2014) 211 (1):89–104. doi: 10.1084/jem.20130301
38. Stockinger B, Omenetti S. The Dichotomous Nature of T Helper 17 Cells. *Nat Rev Immunol* (2017) 17(9):535–44. doi: 10.1038/nri.2017.50
39. Mackay LK, Rahimpour A, Ma JZ, Collins N, Stock AT, Hafon M-L, et al. The Developmental Pathway for CD103+CD8+ Tissue-Resident Memory T Cells of Skin. *Nat Immunol* (2013) 14(12):1294–301. doi: 10.1038/ni.2744
40. Sathaliyawala T, Kubota M, Yudanin N, Turner D, Camp P, Thome, Joseph JC, et al. Distribution and Compartmentalization of Human Circulating and Tissue-Resident Memory T Cell Subsets. *Immunity* (2013) 38(1):187–97. doi: 10.1016/j.immuni.2012.09.020
41. Thome, Joseph JC, Yudanin N, Ohmura Y, Kubota M, Grinshpun B, Sathaliyawala T, et al. Spatial Map of Human T Cell Compartmentalization and Maintenance Over Decades of Life. *Cell* (2014) 159(4):814–28. doi: 10.1016/j.cell.2014.10.026
42. Kumar BV, Ma W, Miron M, Granot T, Guyer RS, Carpenter DJ, et al. Human Tissue-Resident Memory T Cells Are Defined by Core Transcriptional and Functional Signatures in Lymphoid and Mucosal Sites. *Cell Rep* (2017) 20 (12):2921–34. doi: 10.1016/j.celrep.2017.08.078
43. Mackay LK, Kallies A. Transcriptional Regulation of Tissue-Resident Lymphocytes. *Trends Immunol* (2017) 38(2):94–103. doi: 10.1016/j.it.2016.11.004
44. Klicznik MM, Morawski PA, Hollbacher B, Varkhande SR, Motley SJ, Kuri-Cervantes L, et al. Human CD4(+)CD103(+) Cutaneous Resident Memory T Cells Are Found in the Circulation of Healthy Individuals. *Sci Immunol* (2019) 4(37):1–15. doi: 10.1126/sciimmunol.aav8995
45. Wong MT, Ong DE, Lim FS, Teng KW, McGovern N, Narayanan S, et al. A High-Dimensional Atlas of Human T Cell Diversity Reveals Tissue-Specific Trafficking and Cytokine Signatures. *Immunity* (2016) 45(2):442–56. doi: 10.1016/j.immuni.2016.07.007
46. Park CO, Fu X, Jiang X, Pan Y, Teague JE, Collins N, et al. Staged Development of Long-Lived T-Cell Receptor Alphabeta TH17 Resident Memory T-Cell Population to Candida Albicans After Skin Infection. *J Allergy Clin Immunol* (2018) 142(2):647–62. doi: 10.1016/j.jaci.2017.09.042
47. Collin M, Bigley V. Human Dendritic Cell Subsets: An Update. *Immunology* (2018) 154(1):3–20. doi: 10.1111/imm.12888
48. Natsuaki Y, Egawa G, Nakamizo S, Ono S, Hanakawa S, Okada T, et al. Perivascular Leukocyte Clusters Are Essential for Efficient Activation of Effector T Cells in the Skin. *Nat Immunol* (2014) 15(11):1064–9. doi: 10.1038/ni.2992
49. Collins N, Jiang X, Zaid A, Macleod BL, Li J, Park CO, et al. Skin CD4(+) Memory T Cells Exhibit Combined Cluster-Mediated Retention and Equilibration With the Circulation. *Nat Commun* (2016) 7:11514. doi: 10.1038/ncomms11514
50. Lin AM, Rubin CJ, Khandpur R, Wang JY, Riblett M, Yalavarthi S, et al. Mast Cells and Neutrophils Release IL-17 Through Extracellular Trap Formation in Psoriasis. *J Immunol* (2011) 187(1):490–500. doi: 10.4049/jimmunol.1100123
51. Keijsers R, Hendriks AGM, van Erp PEJ, van Cranenbroek B, van de Kerkhof PCM, Koenen H, et al. In Vivo Induction of Cutaneous Inflammation Results in the Accumulation of Extracellular Trap-Forming Neutrophils Expressing RORgammat and IL-17. *J Invest Dermatol* (2014) 134(5):1276–84. doi: 10.1038/jid.2013.526
52. Wang Z, Mascarenhas N, Eckmann L, Miyamoto Y, Sun X, Kawakami T, et al. Skin Microbiome Promotes Mast Cell Maturation by Triggering Stem Cell Factor Production in Keratinocytes. *J Allergy Clin Immunol* (2017) 139 (4):1205–16.e1206. doi: 10.1016/j.jaci.2016.09.019
53. Wu CC, Kim JN, Wang Z, Chang YL, Zengler K, Di Nardo A. Mast Cell Recruitment Is Modulated by the Hairless Skin Microbiome. *J Allergy Clin Immunol* (2019) 144(1):330–3.e336. doi: 10.1016/j.jaci.2019.02.033
54. Buckland J. New Role for Mast Cells as IL-17-Expressing Effector Cells in Established RA. *Nat Rev Rheumatol* (2010) 6(5):243. doi: 10.1038/nrrheum.2010.50
55. Hueber AJ, Asquith DL, Miller AM, Reilly J, Kerr S, Leipe J, et al. Mast Cells Express IL-17A in Rheumatoid Arthritis Synovium. *J Immunol* (2010) 184 (7):3336–40. doi: 10.4049/jimmunol.0903566
56. Kenna TJ, Brown MA. The Role of IL-17-Secreting Mast Cells in Inflammatory Joint Disease. *Nat Rev Rheumatol* (2013) 9(6):375–9. doi: 10.1038/nrrheum.2012.205
57. Liu X, Jin H, Zhang G, Lin X, Chen C, Sun J, et al. Intratumor IL-17-Positive Mast Cells Are the Major Source of the IL-17 That Is Predictive of Survival

in Gastric Cancer Patients. *PloS One* (2014) 9(9):e106834. doi: 10.1371/journal.pone.0106834
58. Chen SJ, Duan YG, Haidl G, Allam JP. Predomination of IL-17-Producing Tryptase-Positive/Chymase-Positive Mast Cells in Azoospermic Chronic Testicular Inflammation. *Andrologia* (2016) 48(6):617–25. doi: 10.1111/and.12487
59. Brembilla NC, Stalder R, Senra L, Boehncke WH. IL-17A Localizes in the Exocytic Compartment of Mast Cells in Psoriatic Skin. *Br J Dermatol* (2017) 177(5):1458–60. doi: 10.1111/bjd.15358
60. Hobo A, Harada K, Maeda T, Uchiyama M, Irisawa R, Yamazaki M, et al. IL-17-Positive Mast Cell Infiltration in the Lesional Skin of Lichen Planopilaris: Possible Role of Mast Cells in Inducing Inflammation and Dermal Fibrosis in Cicatricial Alopecia. *Exp Dermatol* (2020) 29(3):273–7. doi: 10.1111/exd.13816

Conflict of Interest: DR, TN, and LG are employees of Pierre Fabre Dermo-Cosmétique (PFDC).

The remaining authors declare that the research was conducted in the absence of any commercial or financial relationships that could be construed as a potential conflict of interest.

Publisher's Note: All claims expressed in this article are solely those of the authors and do not necessarily represent those of their affiliated organizations, or those of the publisher, the editors and the reviewers. Any product that may be evaluated in this article, or claim that may be made by its manufacturer, is not guaranteed or endorsed by the publisher.